Colloidal Nature of Star Polymer Dilute and Semidilute Solutions

William D. Dozier,[1] John S. Huang, and Lewis J. Fetters*

Corporate Research Laboratory, Exxon Research and Engineering Company, Annandale, New Jersey 08801

Received April 9, 1990; Revised Manuscript Received November 27, 1990

ABSTRACT: The structure of dilute and semidilute solutions of 8-, 12-, and 18-arm star-branched polyisoprenes and 12-arm polystyrenes in good solvent conditions was studied by small-angle neutron scattering (SANS). Interparticle interactions influence the low-angle scattering at concentrations well below the overlap concentration, c^*. We have found in the semidilute solutions evidence for interparticle repulsion and a corresponding depression in the structure factor $S(q)$ at low q. A function for fitting the scattering data from stars is introduced which allows a precise determination of the radius of gyration even at concentrations that are a finite fraction of c^*. The method was also used to fit results from computer simulations and its usefulness compared to the commonly used Kratky plot method.

Introduction

Branched polymers having all branches emanating from the center of the macromolecule are commonly called star polymers. The utilization of modern anionic polymerization techniques has resulted in the preparation of such model materials with arm functionalities ranging from 3 to 270.[2,3] These polymers have been of both experimental and theoretical interest. Experimental work has included melt rheological studies[4-6] and the evaluation of the size parameters in good solvents and under Θ conditions.[2,3,7-12] Neutron spin echo spectroscopy has recently been used to address the topic of star polymer dynamics in dilute solution,[15,16] while small-angle neutron scattering (SANS) measurements have been used[17-19] to determine chain dimensions in the dilute and melt states. From the theoretical view these model branched systems have been useful in the evaluation of scaling concepts,[20] Monte Carlo techniques,[21,22] simulation approaches,[23,24] and renormalization group calculations.[25-27]

Stars have also been of interest as a model system to study polymer colloidal stabilization and as a liquid-state system in their own right where an intriguing soft-core logarithmic repulsion has been suggested.[28] In this paper we present results from SANS experiments on star-branched polyisoprenes (8, 12, and 18 arms) and polystyrene (12 arms) in good solvents. We, in turn, discuss the commonly used methods for determining the star radius of gyration (R_G) and show that interstar interactions cannot be ignored even at dilutions well below the nominal overlap concentration c^* (where c^* is taken as $[\eta]^{-1}$, the inverse of the intrinsic viscosity of the solution).

The measured scattering intensity, $I(q)$, as a function of the scattering wave vector q [$=4\pi/\lambda \sin(\theta/2)$, where λ is the incident neutron wavelength and θ is the scattering angle] can be represented as the product $S(q)P(q)$. Here $S(q)$ represent the interparticle structure factor determined by the interaction potential between the star molecules, while $P(q)$ represents the form factor of the individual stars determined by the structure of the star molecule. For a dilute solution, the interactions between stars are negligible, so $S(q) = 1$, and the intensity $I(q) \sim P(q)$. Knowing $P(q)$ for the individual stars with a selective labeling scheme described later in the paper, we can deduce the structure factor $S(q) = I(q)/P(q)$ at all concentrations. This allows us to measure the effect of the interstar interaction.

The data presented for semidilute solutions show strong evidence for interparticle repulsions [i.e., a depression in the interparticle structure factor $S(q)$ at low q] but no evidence for the anticipated[28] liquid-like ordering [i.e., no peak in $S(q)$]. When partially labeled solutions of stars were studied, the unexpected observation was made that the individual star form factor, $P(q)$, does not change appreciably as a function of polymer concentration up to at least an order of magnitude in excess of c^*.

Experimental Section

The procedures used to prepare and characterize the polyisoprene and polystyrene stars are described elsewhere.[11,29,30] For the polyisoprene stars, the polymerization conditions led to a statistically uniform stereoirregular chain microstructure (~6% 3,4; ~78% cis-1,4; ~16% trans-1,4). The deuterated 12-arm polystyrene star was prepared for this work and was designed to match PS-6-12 in functionality and molecular weight. This objective was achieved.[16] The molecular characteristics of the stars are given in Table I.

The star polyisoprene solutions were prepared in perdeuterated cyclohexane. The samples were in 1 mm path length quartz scattering cells so that the transmission coefficients were typically above 75%. Data were collected for the appropriate solvent in the same path length cell as the samples, and then this was subtracted from the sample' data, with correction for the slightly different transmissions. There was always a small constant background that could not be removed. The incoherent scattering from the PI was negligible due to the low-volume fractions studied.

The polystyrene stars were prepared as blend samples with varying overall polymer concentrations (0.5–10.0%) but with the volume fraction of deuterated stars held constant at 0.5%. A mix of deuterated and ordinary toluene was prepared so that its coherent neutron scattering length density would match that of the protonated stars. The results of those experiments were compared to the scattering from solutions of only the partially deuterated stars. The range in scattering wave vector $q = (2\pi/\lambda) \sin(\theta/2)$, where θ is the scattering angle, was ~0.13–1.5 nm^{-1}.

The SANS experiments (at room temperatures) were done at Brookhaven National Laboratory (BNL) and the National Institute of Standards and Technology (NIST). Several runs were conducted at these facilities. Typical sample-to-detector distance is about 2–3 m; typical wavelength is about 0.6 nm. The spead in wavelength is typically 10% at BNL, 20% at NIST. The q range obtainable at both institutions was comparable.

Results and Discussion

Some of the SANS data for the dilute star solutions are shown in Figure 1. The distinctive shape of the scattering spectrum from the stars is evident in comparison to that of a linear polyisoprene of similar molecular weight (Figure 2). This shape is due to the existence of two important length scales in the star solution, while the linear polymer

0024-9297/91/2224-2810$02.50/0

Table I
Molecular Characteristics of Chlorosilane-Linked Stars

sample	$M_w \times 10^{-4}$, g mol^{-1}	f^a	R_G, nm	ref
PI-8-VIII	4.1	8.0		3
PI-12-VII	25.0	11.9	7.3[b]	3, 17
PI-18-V	357	17.9	50.0[c]	3
PI-18-IX	680	17.4	70.0[c]	3
PS-5-12 (h_8)	14.9	11.8	7.3[d]	11, 13, 14
PS-6-12 (d_8)	14.9	11.6		this work

[a] Average star functionality. [b] Neutron scattering in d_6-benzene. [c] Light scattering in cyclohexane. [d] Neutron scattering in d_8-toluene.

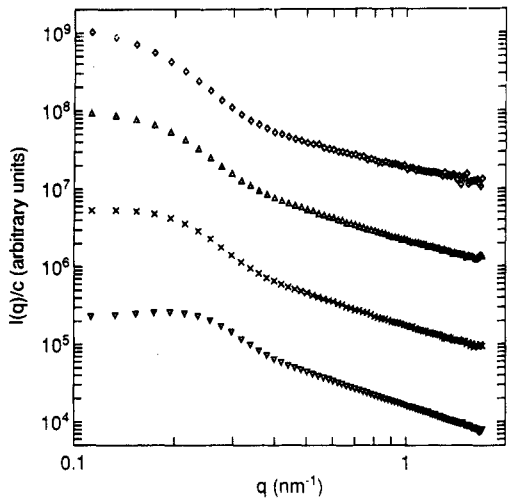

Figure 1. SANS data from 12-arm PI stars (PI-12-VII) in *d*-cyclohexane (◇ = 0.2%; △ = 0.5%, × = 1%; ▽ = 2%). Data are offset by multiplicative constant for visibility.

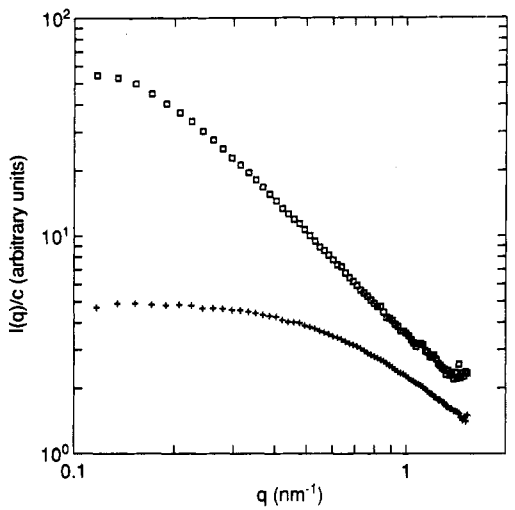

Figure 2. SANS data from linear PI, MW = 25 000 in *d*-cyclohexane (□ = 1%; + = 10%).

solution has but one [either its radius of gyration (R_G) in dilute solution or blob radius (ξ) in a semidilute solution]. The reason for this is that the star, even in dilute solution, can be thought of as a region of semidilute polymer solution surrounded by pure solvent. Hence, the scattering at low wave vector q will essentially look like the scattering from spheres with a radius given by the radius of gyration of the star, while at high q the scattering will look like that from a semidilute polymer solution with its characteristic power law decay in $I(q)$. The exponent characterizing this power law will depend upon the quality of the solvent and will be $-1/\nu$, where ν is the Flory exponent. At Θ conditions, the polymer is nearly an ideal random walk ($\nu = {}^1/_2$), and the exponent then is -2. For a good solvent, $\nu = {}^3/_5$ (self-avoiding random walk) and the scattering falls off as $q^{-5/3}$. In stars, this behavior is complicated by the expected stretching of the arms, which will be especially important for stars with relatively short arms, while stars with very high molecular weight should at large q ($qR_G \gg 1$) exhibit scattering exactly like that of a semidilute solution of linear polymer.

Table II
Neutron Scattering Based Radii of Gyration for Polyisoprene Stars as a Function of Concentration

sample	concn, g dL^{-1}	$P(q)^a$ R_G, nm	Guinier R_G, nm	Kratky[b] R_G (star), nm	Kratky R_G (arm), nm
PI-8-VIII	1.0	4.28	3.93	4.91	
	5.0		2.78	3.21	
	9.0		1.92		
	10.0		1.36		
PI-12-VII	0.05	10.54	10.0	11.81	7.02
	0.08	10.48	10.2	12.94	7.69
	0.10	10.95	9.7	11.82	7.02
	0.13	10.17	9.6	12.89	7.66
	0.20	11.05	9.2	11.58	6.88
	0.50	9.56	8.5	10.37	6.16
	1.00	7.73	6.9	8.97	5.33
	1.30		6.0	8.55	5.08
	2.00		4.8	7.74	4.60
	2.70			6.36	3.78
	4.00			5.62	3.34

[a] $P(q)$ is given by eq 5. [b] Kratky values were obtained from the peak position of the Kratky plots.

The commonly used method of determining the radius of gyration of stars has been the use of "Kratky plots", the peak of which determines a scaling length (taken to be R_G for one arm of the star),[17] which comes from the formalism due to Benoit.[31] In the so-called Kratky plots the scattered intensity is multiplied by a power of the wave vector $q^{-1/\nu}$ and plotted against the wave vector q. For the case of a Gaussian star, ν is ${}^1/_2$, so $I(q)q^2$ is plotted against q in the Kratky plot. Once this single-arm R_G is determined from the Kratky plot, R_G for the star is taken to be[20]

$$R_G^{\text{star}} = R_G^{\text{arm}}\left[\frac{3f-2}{f}\right]^{1/2} \quad (1)$$

in good solvent where f is the number of arms. While these approaches have been helpful either in gaining qualitative understanding[13] or in obtaining a length for scaling purposes,[20] the quantitative agreement of $I(q)$ with any theoretical function has typically been poor. In addition, the Kratky plot method is strictly valid only for Gaussian chains; its applicability to the good solvent case has not been established.

The scattering spectra for the dilute solutions can be treated with a Guinier approximation for small q

$$I(q) = I(0)\exp\left[-\tfrac{1}{3}q^2R_G^2\right] \quad (2)$$

($qR_G \ll 1$) to obtain R_G. In Table II, the R_G values obtained by the Guinier fit and by the Kratky plot method are given as a function of polymer concentration. The crossover concentrations of the 8-VIII and 12-VII stars are found (in ref 13) as 4.0% and 1.7%, respectively. Note that even at concentrations well below c^*, the measured R_G is not independent of concentration and that the Kratky plot data are systematically higher than the data obtained by the Guinier fit.

Computer simulations of stars in good solvents have been done,[23] and the values obtained are given in Table III. Here we can compare the various methods for determining R_G without any interparticle effects (the simulations were on single stars). All methods agree with

Table III
Simulation Results for Stars

length	f^a	simulation[23]	$P(q)^b$	Guinier R_G, nm	Kratky[c] (star), nm	Kratky (arm), nm
50	10	1.01	1.04	1.00	1.06	0.64
50	20	1.12	1.15	1.12	1.30	0.76
50	30	1.22	1.26	1.23	1.64	0.96
50	40	1.34	1.36	1.33	1.64	0.96
100	10	1.51	1.58	1.43	1.60	0.96
200	10	2.34	2.39	2.18	3.20	1.91

[a] f is the average functionality of the star. [b] $P(q)$ is given by eq 5. [c] Kratky values were obtained from the peak position of the Kratky plots.

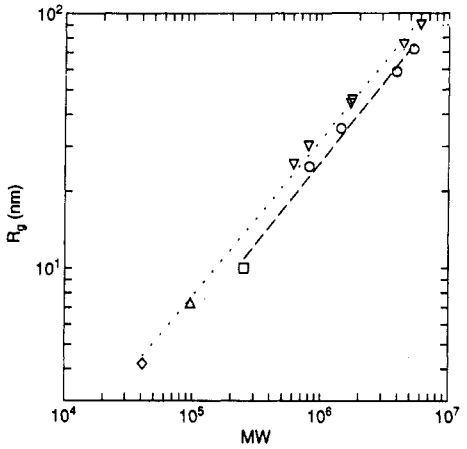

Figure 3. R_g vs MW for PI-12-VII (□, this work; ○, light scattering data from ref 3) and PI-8-VIII (◇, R_g from Kratky plot ref 17; △, this work; ▽, light scattering data from ref 3). Dashed lines are fits to power law with $\nu = 0.6$.

the simulation result for the smallest star (10 arms, 50 links), but for all of the other simulations the Kratky method is the worst fit, always overestimating R_G. Note that the discreteness of the real scattering data causes the value of q_{peak} to have relatively large uncertainty if it is determined graphically, and since the function from which the relationship ($q_{peak}R_G = 1.2$) is derived does not fit the data well, one cannot expect to get a better value by interpolation.

In Figure 3 data of refs 3 and 17 are shown along with the values for R_G (taken to be the limit of zero concentration of the Guinier values) from Table II. The scaling exponent for both lines, including data from both light scattering and SANS, is about 0.6. The result of 0.55 determined in ref 3 is no doubt due to the limited range of data points and is therefore not inconsistent with our results.

The effect of interstar interactions on the measurements of R_G can be readily seen by referring to Table II. The data show that measuring R_G at half of c^* will result in a 30% underestimation of R_G and that a 10% effect is still present at $c^*/10$. This is due to a repulsive interaction between the stars discussed below.

To develop an analytical expression for fitting the star scattering spectra, we identify two regimes in q. For small q, the scattering should look like that from spherical objects of radius R_G. For large q, the scattering should be like the large-angle scattering from a semidilute polymer solution; i.e., it should look like the scattering from a power law density correlation function with the power derived from the exponent ν. We propose a functional description of the scattering that is just the sum of two terms, the first of which is the small q scattering from the spherical stars and the second is the Fourier transform of the mass–mass

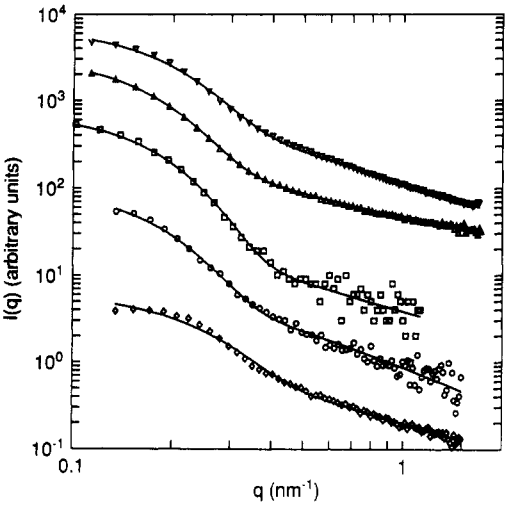

Figure 4. SANS data for PI-12-VII in d-cyclohexane with analytical $P(q)$ fits (○ = 0.05%; □ = 0.08%; △ = 0.1%; ▽ = 0.2%; ◇ = 1%). Data are offset by multiplicative constant for visibility.

correlation function inside the star. This becomes

$$I(q) = I(0)\exp\left[-\frac{1}{3}q^2R_G^2\right] + \frac{4\pi\alpha}{q}\int_0^{\xi} rg(r)\sin qr\,dr \quad (3)$$

where ξ is the correlation length inside the star, or equivalently the radius of the outermost blobs ($\xi = 2R_G/\sqrt{f}$),[20] and α is a constant to be determined (it should not be a function of the polymer concentration as the second term is that of a semidilute solution). Note that since we have at most 12 arms here, ξ/R_G is of order unity and the largest blobs contribute almost all of the scattering (if this were not so, we would have to average the second term over the various blob radii). The integral cuts off at ξ because the correlation function $g(r)$ is constant for $\xi < r < R_G$. Since the star is not expected to have a sharp cutoff but rather a somewhat fuzzy edge, we took a Gaussian cutoff for the "sphere". The particular form of the first term was chosen to keep consistency with the Guinier expansion. The mass correlation function $g(r)$ was taken to be[20]

$$g(r) = r^{1/\nu-3} \quad (4)$$

where $r < \xi$. For fitting eq 3 to the data from computer simulations of our SANS data, we used $\nu = {}^2/_3$ expecting the arms of these rather small stars to be somewhat stretched. We did not allow ν to vary since there would be a strong correlation between ν and the small (but variable) background term in the SANS data which was necessary because of fluctuations in the neutron beam intensity. Because of the necessity of fitting the background, we could not determine ν for the 12-VII or 8-VIII samples, and, in fact, good fits could be obtained with $0.4 < \nu < 0.8$. Using $\nu = {}^1/_2$, we could also fit previously published data for the PS stars in Θ conditions (below). To avoid doing a numerical integration for eq 3, we inserted a factor of $\exp(-r/\xi)$ in the integrand and integrated to infinity. The integration could then be done to yield

$$I(q) \propto I_0\exp\left[-\frac{1}{3}q^2R_G^2\right] + \frac{4\pi\alpha}{q\xi}\frac{\sin\left[\mu\tan^{-1}(q\xi)\right]}{[1+q^2\xi^2]^{\mu/2}}\Gamma(\mu) \quad (5)$$

where μ is $1/(\nu-1)$ and $\Gamma(\mu)$ is the gamma function with argument μ. The fits in Figures 1 and 4 were obtained by using a Levenberg–Marquardt algorithm for the nonlinear least-squares fit. Note that since $I(q)$ for these samples does not fall off as q^{-2} at high q, there is no possibility of

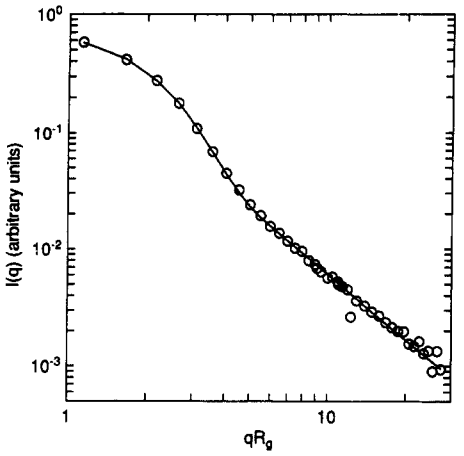

Figure 5. SANS data from ref 13 for PS-6-12 stars in Θ solvent (q axis is scaled by their R_g determined by Kratky plot) with fit to analytical $P(q)$.

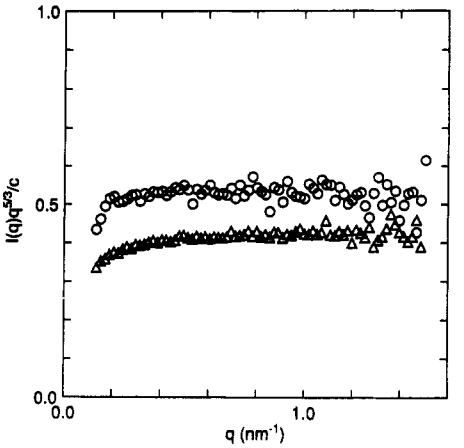

Figure 6. Generalized Kratky plot of SANS data for high MW 18-arm PI stars (○ = 0.5%; PI-18-IX; △ = 1.0%; PI-18-V).

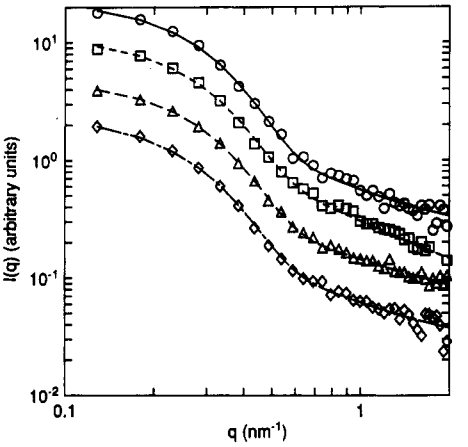

Figure 7. SANS data from contrast-matched blend solutions of several total polymer concentrations, the concentration of labeled polymer held constant at 0.5% (○ = 1%; □ = 1.5%; △ = 2.5%; ◇ = 10%). Data are offset by multiplicative constant for visibility.

using the Benoit expression[31] to even get a qualitative treatment of the data. This is to be expected for non-Gaussian stars. It should be pointed out that this function is chiefly useful for accurately determining R_G and it is not very sensitive to f (because ξ is not very sensitive to f), nor is it a good way of finding ν (since typical data will be of the appropriate q range for determining either R_G or ν but not both).

In Figure 4 scattering data for various dilute solutions of the 12-VII polyisoprene star are presented along with fits to eq 5. Table II shows that this method is less sensitive to the polymer concentration than either method used. This is presumably because we are fitting the entire scattering curve while the interparticle interactions mainly affect only the first few data points. The R_G obtained from the fits is in excellent agreement with the R_G obtained by extrapolating the Guiner fit results to zero concentration. We applied eq 5 to the simulated stars and again got good agreement as shown in Table III. Figure 5 shows data from ref 13, for PS-6-12 under Θ conditions along with a fit to eq 5 using $\nu = {}^1/_2$. The agreement again is excellent. Our value for R_G from the fit is 0.86 (for their scaled data), showing that the Kratky method overestimated R_G by about 14% or that the data were not taken at exactly Θ conditions.

For the high molecular weight 18-arm stars used in this study, the q range available to us was not sufficient to see the effect of the spherical shape of the star, but we could get a good look at the scaling region. In Figure 6 the scattering spectra of the 18-arm stars are shown plotted in "generalized Kratky" plots. Instead of q^2, $I(q)$ was multiplied by $q^{5/3}$. The flatness of the curves show that these large stars nicely exhibit the ideal self-avoiding chain behavior ($\nu = {}^3/_5$).

In Figure 7, the scattering spectra are shown for blend solutions of various total polymer concentrations where the volume fraction of deuterated polystyrene stars is constant at 0.5%. Since the d/h-toluene mixture (4% deuterated) was chosen to match the protonated polystyrene, all of the coherent scattering comes from the deuterated stars. Note that the data have not been scaled by the polymer concentration and that the curves are practically identical. These data show that at least for these rather short-armed 12-arm stars the single particle scattering spectrum is not affected by the total star concentration, even at over twice c^* (4.2% for PS 6-12).[11]

Using the above result, we divided the fitting function for the 0.5% total polymer weight fraction scattering spectrum into SANS data for 1.0%, 3.3%, and 6.7% deuterated PS-6-12 in toluene using $\nu = 0.6$. After scaling by the concentration, no other treatment of the data was performed. Figure 8a shows the $S(q)$ thus obtained for the three samples. Note that at high q $S(q) \rightarrow 1$. While we could get good fits for $P(q)$ for a range of values of ν, only if we took $\nu = 0.6$ could we get this correct behavior. By applying the same treatment of the data for the PI-8-VII stars [fitting the scattering for the lowest concentration and taking the result to be $P(q)$ at all concentrations] we obtained the results in Figure 8b. For this set of data, absolute scattering intensities were unfortunately not available, so the $S(q)$ values were scaled so that $S(q) \rightarrow 1$. Note also the marked "correlation hole" at small q.

Why there should be such a depression of $S(q)$ at $q \rightarrow 0$ without any peak at some mean interstar correlation distance is not obvious. The lack of a peak could be evidence of the "soft-core" nature of the star–star repulsion. It could also be due to the "fuzziness" of the star scattering profile which could act like a polydispersity effect.[32]

Conclusions

We have found that the colloidal nature of star polymer solutions cannot be ignored; thus, care must be taken to anticipate interaction effects. This means, for example, that low-angle light scattering is very difficult for the purpose of measuring R_G, since dust contamination will prevent experiments being done at sufficient dilution to

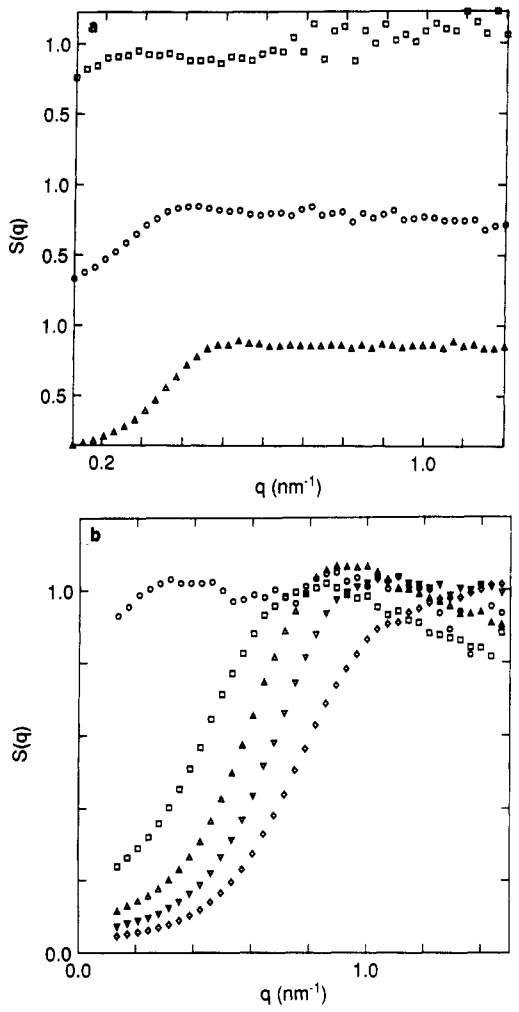

Figure 8. (a) Liquid structure factor $S(q)$ for PS-6-12 stars in *d*-toluene (□ = 1%; ○ = 3.3%; △ = 6.7%). Data are offset by additive constant. (b) Liquid structure factor $S(q)$ for PI-8-VIII stars in *d*-cyclohexane, scaled so that $S(q) \to 1$ (○ = 1%; □ = 5%; △ = 9%; ▽ = 14%; ◇ = 28%).

avoid the effects of interparticle correlations. We see interparticle effects as low as a factor of 20–30 below the nominal c^* in trying to treat the data with a Guinier approximation. We have also shown that the use of a Kratky plot is not an accurate method for determining R_G in good solvents, although it is a convenient means to get a scaling length. We have presented a method of determining R_G that is not as susceptible to interstar correlation effects. This fitting function method works well for the good solvent solutions studied here as well as results from computer simulation and Θ solvent solutions reported elsewhere. The scaling behavior in the tail of the scattering does not change appreciably in solutions with total polymer concentration up to twice c^*. This implies that the changes in $I(q)$ as the star concentration increases were due entirely to interstar correlations.

We observed a marked correlation hole in the interstar structure factor due to the decrease in the isothermal compressibility as the polymer concentration increased. The presence of such a small compressibility without any peak in $S(q)$ is surprising and warrants further study.

Acknowledgment. We thank Benno Schoenborn and Dieter Schneider of BNL and Charles Glinka of NIST for their hospitality and assistance. Helpful discussions of the results with Tom Witten, Michael Cates, and Gary Grest are appreciated as well as the technical assistance of Jim Sung.

References and Notes

(1) Present address: Argonne National Laboratory, Argonne, IL 60439.
(2) Roovers, J.; Toporowski, P.; Martin, J. *Macromolecules* **1989**, *22*, 1897.
(3) Bauer, B. J.; Fetters, L. J.; Graessley, W. W.; Hadjichristidis, N.; Quack, G. F. *Macromolecules* **1989**, *22*, 2337.
(4) Pearson, D. S.; Helfand, E. *Macromolecules* **1984**, *17*, 888.
(5) Hadjichristidis, N.; Roovers, J. *Polymer* **1985**, *26*, 1087.
(6) Roovers, J. *Polymer* **1985**, *26*, 1091.
(7) Roovers, J.; Martin, J. *J. Polym. Sci., Part B, Polym. Phys.* **1989**, *27*, 2513.
(8) Hadjichristidis, N.; Roovers, J. E. L. *J. Polym. Sci., Polym. Phys. Ed.* **1974**, *12*, 2521.
(9) Bauer, B. J.; Hadjichristidis, N.; Fetters, L. J.; Roovers, J. *J. Am. Chem. Soc.* **1980**, *102*, 2410.
(10) Huber, K.; Burchard, W.; Fetters, L. J. *Macromolecules* **1983**, *16*, 2287.
(11) Khasat, N.; Pennisi, R. W.; Hadjichristidis, N.; Fetters, L. J. *Macromolecules* **1988**, *21*, 1100.
(12) Roovers, J.; Toporowski, P. *J. Polym. Sci., Polym. Phys. Ed.* **1980**, *18*, 1907.
(13) Huber, K.; Bantle, S.; Burchard, W.; Fetters, L. J. *Macromolecules* **1986**, *19*, 1404.
(14) Huber, K.; Burchard, W.; Bantle, S.; Fetters, L. J. *Polymer* **1987**, *28*, 1990, 1997.
(15) Richter, D.; Farago, B.; Fetters, L. J.; Huang, J. S.; Ewen, B. *Macromolecules* **1990**, in press.
(16) Richter, D.; Farago, B.; Huang, J. S.; Fetters, L. J.; Ewen, B. *Macromolecules* **1989**, *22*, 468.
(17) Richter, D.; Stühm, B.; Ewen, B.; Nerger, D. *Phys. Rev. Lett.* **1987**, *58*, 2462.
(18) Horton, J. C.; Squires, G. L.; Boothroyd, A. T.; Fetters, L. J.; Rennie, A. R.; Glinka, C. J.; Robinson, R. A. *Macromolecules* **1989**, *22*, 681.
(19) Boothroyd, A. T.; Squires, G. L.; Fetters, L. J.; Rennie, A. R.; Horton, J. C.; de Vallêra, A. M. B. G. *Macromolecules* **1989**, *22*, 3130.
(20) Daoud, M.; Cotton, J. P. *J. Phys.* **1982**, *43*, 531.
(21) Rey, A.; Freire, J. J.; de la Torre, J. G. *Macromolecules* **1987**, *20*, 342.
(22) Batoulis, J.; Kremer, K. *Macromolecules* **1989**, *22*, 4277.
(23) Grest, G. S.; Kremer, K.; Witten, T. A. *Macromolecules* **1987**, *20*, 1376.
(24) Grest, G. S.; Kremer, K.; Milner, S.; Witten, T. A. *Macromolecules* **1989**, *22*, 1094.
(25) Miyake, A.; Freed, K. F. *Macromolecules* **1983**, *16*, 1228.
(26) Douglas, J. F.; Freed, K. *Macromolecules* **1984**, *17*, 1854.
(27) Douglas, J. F.; Roovers, J.; Freed, K. F. *Macromolecules* **1990**, *23*, 4168.
(28) Witten, T. A.; Pincus, P. A. *Macromolecules* **1986**, *19*, 2509.
(29) Hadjichristidis, N.; Guyot, A.; Fetters, L. J. *Macromolecules* **1978**, *11*, 668.
(30) Hadjichristidis, N.; Fetters, L. J. *Macromolecules* **1980**, *13*, 191.
(31) Benoit, H. *J. Polym. Sci.* **1953**, *11*, 561.
(32) Kotlarchyk, M.; Chen, S. H. *J. Chem. Phys.* **1983**, *79*, 2461.

Registry No. SANS, 12586-31-1; polyisopyrene, 9003-31-0; polystyrene, 9003-53-6.